Domain coexistence in nonlinear optical pattern formation

Svetlana L. Lachinova and Weiping Lu
Department of Physics, Heriot-Watt University, Edinburgh, EH14 4AS, United Kingdom
(Received 15 March 2001; published 17 July 2001)

We report on domain coexistence of a variety of different modes in a two-dimensional nonlinear optoelectronic model. The changes of stabilities of these modes are shown to give rise to new forms of spatial and spatiotemporal structures. The existence of these domain patterns explains some of the patterns recently observed in an optical system with a large array optoelectronic feedback circuit.

DOI: 10.1103/PhysRevE.64.026207 PACS number(s): 05.45.−a, 42.65.Sf, 89.75.Kd

It is now well known that dissipative structure emerges from nonlinear interaction and under symmetry constraints in spatially extended systems in diverse areas such as fluid, chemistry, biology, and optics [1]. Most studies of pattern formation began in the earlier years with the limiting cases, in which coherent structure appears due to a single spatial mode born from instabilities of the homogeneous steady state and the complexity in the system evolves from the subsequent instabilities of this mode. This mechanism is responsible for dissipative structures observed in some best-known pattern-forming systems, such as Couette-Taylor flow, Rayleigh-Bénard convection, electroconvection, and two-level broad-area lasers. Recently, there has been a considerable interest in pattern formations that arise from a few numbers of nonlinearly interacting modes or elementary patterns. In this case new types of patterns have been observed, arising from resonant interactions of these excited modes with different wave numbers and orientations [2,3]. Flower patterns and superlattice structures are such examples that have been reported by many authors [4–9]. Another class of pattern formation for this case is domain coexistence of these modes, that is, patterns of different symmetry and/or different wave numbers can coexist in different domains of the available space [10,11]. The boundaries of the domains are commonly referred to as domain walls [12]. The simplest case of domain coexistence corresponds to bistable situations involving two modes, such as rolls and hexagons in Rayleign-Bénard convection [13] and in optical systems [14]. Complex domain structures have been more recently observed in experiments [15–17].

In this article we present an investigation of domain coexistence of a variety of different elementary patterns in a two-dimensional optical system with periodic nonlinearity. We show the coexistence of interacting modes in the parameter regions of unstable homogeneous steady state solutions of the system. The changes of stabilities of these modes on the variations of the input light intensity are found to give rise to a sequence of spatial bifurcations, from which new forms of spatial structures develop. The predicted domain patterns in the theory can explain some of the spatial structures observed in the experiment [18].

A broad-area nonlinear optoelectronic feedback system has recently been shown to display a kaleidoscope of patterns [18]. The experimental system under investigation is a generic (transversely) two-dimensional hybrid optoelectronic device comprising a phase spatial light modulator (SLM) coupled with a photo-detector array through a combined optical and electronic feedback loop. A schematic is shown in Fig. 1. The phase of the coherent input wave is modulated as it transmits through the SLM, the phase modulations in the transverse space being linearly proportional to the control intensity of the SLM in local regions. The input wave then experiences a free propagation, and subsequently nonlinearity and spatial spectral filtering through the electronic signal processing before it is fed back to the SLM. The optical and electronic interfacing is provided by the photoarray in the feedback loop. Pattern formations have been observed in experiments with a variety of nonlinearities for which the electronic signal processor has been programmed, ranging from cubic, unimodal, to bimodal. Interestingly, different forms of nonlinearities have been shown to exhibit many common features in pattern formations. In this work we choose the phase modulation in the signal processor to be cosine type, similar to the bimodal-type nonlinearity in the experiment. From a theoretical point of view, the experimental system can be accurately modeled by a set of coupled partial differential equations. The dynamics of the phase variations $u(\mathbf{r},t)$ in the nonlinear system is described by the following equation,

$$\frac{\partial u(\mathbf{r},t)}{\partial t}+u(\mathbf{r},t)=D\nabla_{\perp}^{2}u(\mathbf{r},t)+Kw_{FB}(\mathbf{r},t), \qquad (1)$$

where $\mathbf{r}$ is the radius vector in the transverse plane, t is the time coordinate normalized to the characteristic relaxation time of the nonlinearity τ_0, D is the diffusion coefficient, $\nabla_{\perp}^{2}$ the transverse Laplacian, and K the feedback gain coefficient. The feedback signal w_{FB}, which is given as

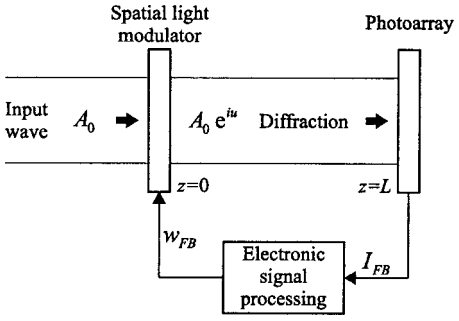

FIG. 1. A schematic of the nonlinear optoelectronic feedback system.

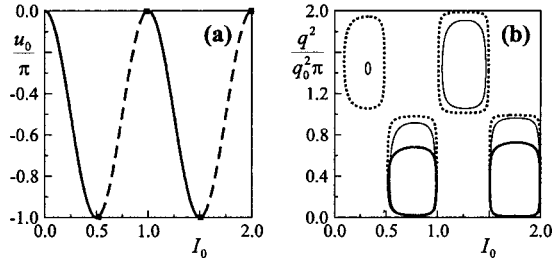

FIG. 2. (a) Homogeneous steady state solution, solid and dashed segments correspond to stable and unstable solutions, respectively. (b) Instability island; areas surrounded by dotted, thin, and thick solid loops correspond to three different cases: $D=0$ and without spatial frequency filtering, $D=1/q_0^2$ and without spectral filtering, and $D=0$ and with spectral filtering $q_{cut}=0.735\sqrt{\pi}q_0$, $\alpha=8$, respectively. The *xy* arrangement in the bifurcation plot in (b) provides a better visual relation to (a). The feedback gain coefficient $K=-0.5\pi$ is consistent with experimental arrangement.

$$w_{FB}(\mathbf{r},t)=\int [1-\cos(2\pi I_d)]h(\mathbf{r}-\mathbf{r}')d^2\mathbf{r}', \qquad (2)$$

is a convolution integral of cosine function of $I_d(\mathbf{r},t)$ and $h(\mathbf{r})$. Here $I_d(\mathbf{r},t)=|A(\mathbf{r},z=L,t)|^2$ is the intensity distribution of the light wave after a free propagation of length L and h a low-pass spatial filter in the super-Gaussian shape with the cutoff frequency q_{cut} and power α. The Fourier transform of h is therefore $H(q)=\exp[-(|\mathbf{q}|/q_{cut})^{\alpha}]$. The free propagation of the light between $z=0$, and $z=L$ along the longitudinal axis is described by the equation

$$-2ik_0\frac{\partial A(\mathbf{r},z,t)}{\partial z}=\nabla_{\perp}^2 A(\mathbf{r},z,t) \qquad (3)$$

and the boundary condition $A(\mathbf{r},z=0,t)=A_0\exp[iu(\mathbf{r},t)]$, where A_0 is the amplitude of the incident optical wave and k_0 is its wave number.

Equations (1)–(3) admit a spatially homogeneous steady state solution $u_0=K[1-\cos(2\pi I_d)]$ and $I_d=I_0\equiv|A_0|^2$, as shown in Fig. 2(a). The linear stability analysis of these equations gives the characteristic equation

$$\lambda=-(1+Dq^2)+2K\sin(2\pi I_0)2\pi I_0\sin(q^2/q_0^2)\times\exp[-(|\mathbf{q}|/q_{cut})^{\alpha}], \qquad (4)$$

where q is the perturbation wave number and $q_0=\sqrt{2k_0/L}$. $\lambda=0$ marks a bifurcation point from which the homogeneous steady state looses its stability and gives rise to static pattern formation. The condition $\partial\lambda/\partial q=0$ for $\lambda\geqslant 0$ from the above equation determines the wave numbers that correspond to the maximum gain modes at and above the threshold, referred to as the critical wave number q_c. q_c is dependent on the input wave intensity I_0 and other parameters of the system. However, in the absence of diffusion, i.e., $D=0$, q_c that is given by the transcendental equation $\tan(q_c^2/q_0^2)=2q_{cut}^{\alpha}/\alpha q_c^{\alpha-2}$ does not depend on I_0. For the parameters given in Fig. 2, $q_c\approx\sqrt{0.336\pi}q_0$. This is one of the basic wave numbers observed throughout in our simulations detailed below. In the absence of both diffusion and filtering, q_c has a simpler form of $\sqrt{(1/2+n)\pi}q_0$, $n=0,1,2,\ldots$. As seen from Eq. (4), λ is cyclic both in the intensity I_0 and q^2. This gives a two-dimensional array of instability islands in the (I_0,q^2) space. Figure 2(b) gives the first four instability islands for three different parameter sets. The areas of the islands are the largest in the absence of both diffusion and spatial filtering. Since the both effects provide transverse spatial coupling in the optical/electric waves in the system, we find that, once the frequency cutoff is present, the diffusion does not qualitatively alter the dynamics of the system. For simplicity, D is set to 0 in the following simulations. The low-pass spatial filtering ensures that only first instability islands in the q direction join the dynamical interactions. As a result, instability occurs only in the regions of the steady state solution u_0 where $\partial u/\partial I_0>0$, that is the areas marked by the dashed lines in Fig. 2(a).

To investigate optical pattern formations in the system, we have focused on the parameter region $0.4<I_0<1.1$, which covers the whole unstable region in the first cycle of $u_0(I_0)$ and small areas on both sides of this region. We numerically integrated Eqs. (1)–(3) with initial conditions of homogeneous steady states with random noise. The simulation results, as given in Fig. 3 upper row, show a variety of spatial structures evolving from the homogeneous steady states. Let us describe them in detail. When I_0 is just below the first bifurcation point, localized states of random spatial distributions emerge from sufficiently strong initial noise perturbations [trace (a)]. Once I_0 enters the unstable region, bright hexagonal clusters together with some isolated spots are observed [trace (b)]. On increasing I_0, stripes are formed through connecting the neighboring bright spots [trace (c)]. The lengths of the stripes are short initially but increase with the increase of I_0, as more and more spots are connected into the stripes. The stripes eventually dominate the localized states as more spots join stripes [trace (d)]. The stripes are found to be randomly orientated, reflecting the fact of the randomness of their initiations. On further increasing I_0 forms a new type of pattern, which comprises negative hexagonal elements each centered by a bright spot [trace (e) middle area]. We refer to them as mosaics; somewhat similar to hexagonal superlattice in a viscoelastic liquid [7]. The mosaic elements are showed to form through curving stripes surrounding a localized state. With the increase of I_0 from this value, localized states die out whereas clusters of negative hexagon form, giving rise to netlike patterns [trace (f)]. As I_0 moves further right, domains of perpendicular lines emerge from the seemingly irregular nets [trace (g)]. The domain boundaries are formed by defects, such as imperfect squares and pentagons. When I_0 is eventually increased close to the second bifurcation, negative hexagons disappear and are replaced by a triangle type of pattern [trace (h)]. Beyond this point formations of disordered negative localized states, or black holes, are observed.

We find that all the above patterns are stable in the sense that the structures of these patterns do not change qualitatively with time. In general these patterns are formed after one thousand of the characteristic relaxation time from a set of given initial conditions. After this period, some of these

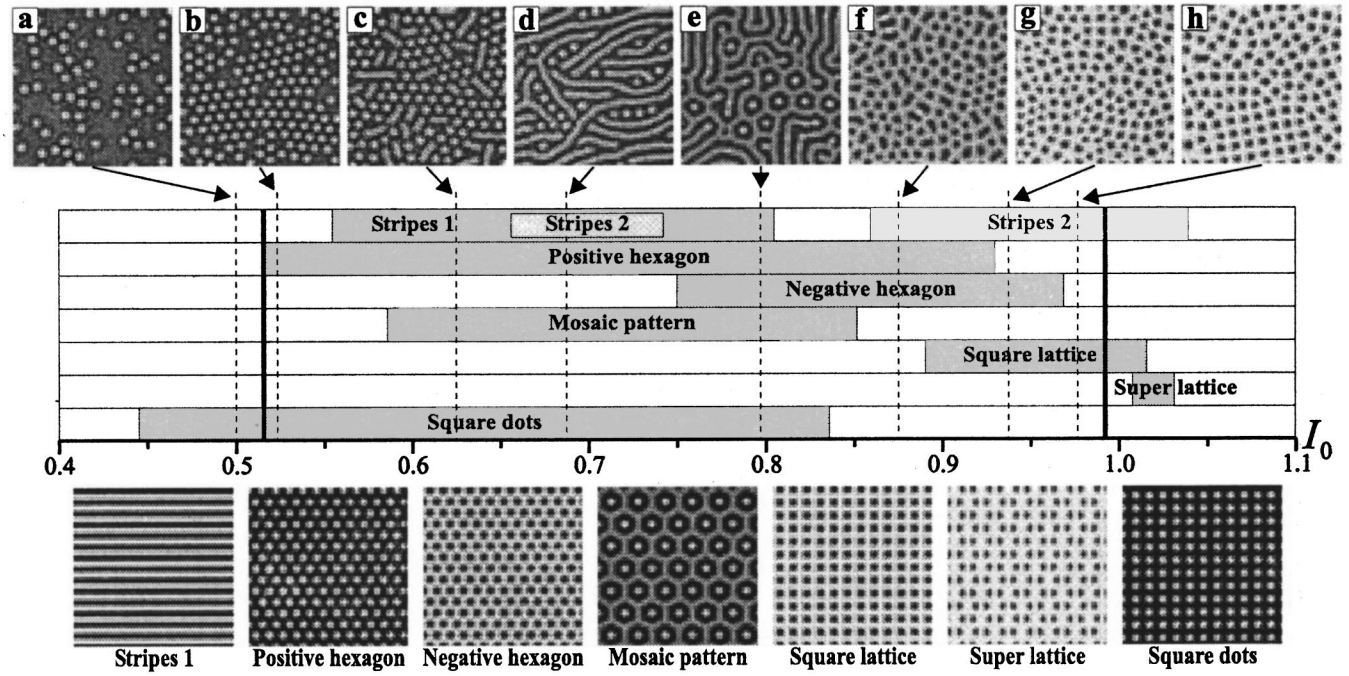

FIG. 3. Domain coexistence of a variety of elementary patterns, obtained by integrating Eqs. (1)–(3) with initial conditions of homogeneous steady states superposed by random noise. Top row: traces (a)–(h) show a consequence of spatial structures on increasing I_0. Middle row: the regions of stable elementary patterns in I_0 axis; the area within the two solid vertical lines corresponds to linearly unstable steady state solution. Bottom row: the spatial structures of the elementary patterns. The parameters used are $D=0$, $q_{cut}=0.735\sqrt{\pi}q_0$, $\alpha=8$, and $K=-0.5\pi$.

patterns [traces (a), (b), (f), (g), and (h)] are completely static, confirmed by measuring the difference between the frames at different times, whereas the others reach dynamical balance, that is, the elements of the patterns may be slightly wobbling in time but overall structure remains unchanged. For the latter case, simulations of $50\,000\tau_0$ have been performed to ensure the patterns observed are not transient. We note that the above observed long transient period for the pattern formation from noisy initial conditions is due to the competition nature of the coexisting elementary patterns, as discussed below. This period reduces to a few hundred τ_0 or less when the final spatial structure comprises only one element, such as rolls or hexagons, for the parameters close to the threshold for pattern formation. All the simulations above have been carried out with grid points 256×256, the results being confirmed by the grid points 512×512. Furthermore, the size of the area in the transverse space is adjusted for optimal simulation results.

How can we explain these irregular and sometimes complex patterns? The presence of clusters of some well-known basic structures has led us to the idea that these patterns may be decomposed into some elementary components or modes. Our first task is therefore to show the existence of various elementary patterns in the system. To do so, we have in our simulation chosen initial conditions that comprise the wave numbers and symmetries of modes obtained from the linear stability analysis and power spectra of the patterns observed. Figure 3 middle row gives the parameter regions for all the elementary patterns numerically observed: stripes, positive and negative hexagons, mosaics, square lattices, superlattices, and square dots. Their corresponding spatial structures are shown in the bottom row of this figure. Different structures are found to coexist in most of the parameter regions investigated due to the multistability of the solutions and their appearance depends on the choice of the initial conditions. The parameter regions for these regular spatial structures were established through a sequence of simulations on increasing (or decreasing) I_0 in small steps, with the last outputs superposed by small noise being used as the current initial conditions.

We find that despite of the diversity of the elementary patterns observed, there are only two basic wave numbers involved in these patterns. The first, q_1, is the critical wave number q_c at the instability threshold (as discussed earlier, q_c is independent on I_0 for the parameter set used here). It corresponds to the stripes 1 in the Fig. 3 middle row and is longer than the second, q_2, the wave number of the stripes 2 (the ratio being 7:6, only stripes 1 is displayed). Both the positive and negative hexagons have the same wave number as q_1, whereas the square lattice is based on the q_2. The latter, in fact, comprises q_2 in two perpendicular directions, $\mathbf{q}_{2,1}$ and $\mathbf{q}_{2,2}$, and the linear combinations $\mathbf{q}_{2,1}\pm\mathbf{q}_{2,2}$, as shown in the spectral wave vector diagram in Fig. 4(a). Here, the second subscript indicates the different directions of the wave vector. The mosaic pattern is made of the both wave numbers, q_1 and q_2. Figure 4(b) shows that the mosaics consist of two positive hexagons of these numbers, the directions being orientated $30°$ with each other. We note that, unlike the 12-fold quasiperiodic structures [2,19], which ex-

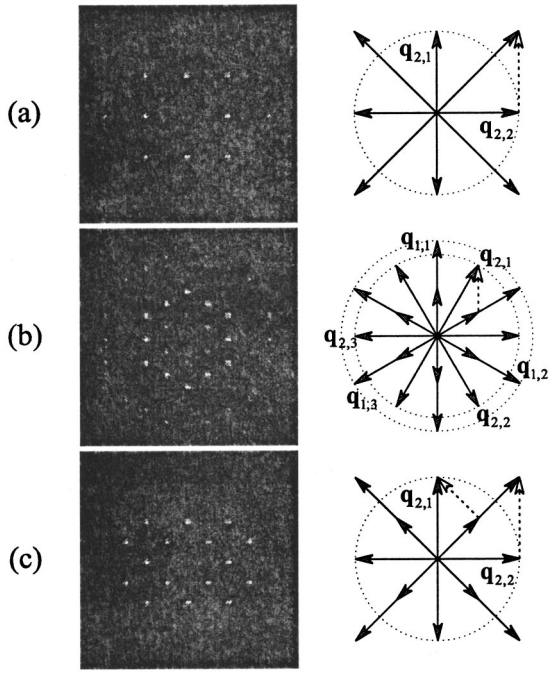

FIG. 4. (a)–(c) are the power spectra (left column) and wave vector diagrams (right column) of the square lattice, mosaic, and superlattice, respectively. The amplitudes of the wave vectors on the right column are increased by a factor of 2 to show more clearly their interactions.

ist in the presence of harmonics of one fundamental unstable mode, the hexagonal families in the mosaics we observe are coupled through the subharmonic $\mathbf{q}_{2,1}=\mathbf{q}_{1,1}/2-\mathbf{q}_{1,3}/2$ [Fig. 4(b)]. The interaction through harmonics is disabled due to the filtering in the feedback. The superlattices are shown to comprise two square lattices, one with wave vectors of $\mathbf{q}_{2,1}$, $\mathbf{q}_{2,2}$, and the other with $(\mathbf{q}_{2,1}\pm\mathbf{q}_{2,2})/2$. They are orientated 45° with each other [Fig. 4(c)] so the combination displays a triangle form. Both mosaic and superlattices patterns are examples of resonant interaction of modes with different values of wave numbers. We note that for the parameters we use, the amplitude equations to the fifth order in the week perturbation expansion are not sufficient for describing these regular spatial structures. This makes bifurcation analysis cumbersome.

The patterns in Fig. 3 upper row can now be clearly explained as domain coexistence of two or more of these elementary patterns. Trace (b) is the coexistence of hexagonal clusters with randomly distributed localized states, whereas traces (c) and (d) is that of localized states and stripes. Trace (e) is made of domains of localized states, stripes, and mosaics while trace (f) comprises negative hexagons and square lattices. Finally, the spatial structure of trace (g) and (h) can be explained by the presence, with different weights, of negative hexagons, square and superlattices, the latter becoming dominate on further increasing I_0. The parameter region for stable superlattices is narrow and is in the area

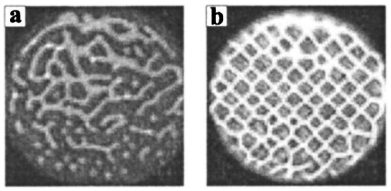

FIG. 5. Domain coexistence observed in the experiment.

where the homogeneous steady states are stable. This structure can be observed from destabilized square lattices on increasing I_0. As we have already mentioned above, all the elementary patterns in the given regions are stable since they are robust to modest amplitude noise perturbations. Because of this, they can be formed even if the initial conditions used in the simulation deviate slightly from the elementary patterns. However, the degree of tolerance to the deviations varies with I_0 so that one pattern is usually more robust than others for a particular value I_0 and the robustness changes with the changes of I_0. This explains why one pattern can dominate others in their domain coexistence. Specifically, for example, the noise level required to destabilize the positive hexagonal solution is higher than that needed for destabilizing the solution of the square dots. Moreover, when the initial conditions deviate from the exact solutions of these two elementary patterns, the convergence rate to the former is found to be faster than that to the latter. This can explain why the square dots are not present in domain coexistence. They are observed only when the positive hexagons are destabilized on decreasing I_0 passing through the first bifurcation point. We note that the elementary components identified in the system are by no means complete but they are sufficient to explain the observed complex patterns. Finally, we have further investigated the effect of the feedback coefficient K on the domain coexistence. We establish that the number of possible elementary patterns decreases on decreasing the values of K. When K is reduced ten times, for example, coexistence of stripes and hexagons are the only patterns obtained in the first cycle of $u_0(I_0)$ [20].

The above simulation and analysis can explain some of the patterns observed in the optical experiment with optoelectronic feedback loop. The experimental setup and experimental results are given in Ref. [18]. The system is well described by our model for the bimodal nonlinearity. Figure 5 comprises two of the observed patterns in the experiment, provided by M. A. Vorontsov. Figure 5(a) shows the experimental evidence of domain coexistence of localized states with stripes. The defected square lattices in Fig. 5(b) can be explained by the coexisting square and superlattices. Moreover, domain coexistence has also been predicted in our theory, as observed in the experiment, using other types of nonlinearities, such as Gaussian, Kerr, and step-wise functions.

Most useful discussions with Dr. M. A. Vorontsov are gratefully acknowledged. This work was supported by EPSRC Research Grant No. Gr/M32573 and the U.S. Army Grant No. R&D8938-PH-01.

[1] See, for example, M. C. Cross and P. C. Hohenberg, Rev. Mod. Phys. **65**, 851 (1993); and L. A. Lugiato, M. Brambilla, and A. Gatti, in *Advances in Atomic Molecular and Optical Physics*, edited by B. Bederson and H. Walther (Academic Press, New York, 1998), Vol. 40, p. 229.
[2] E. V. Degtiarev and M. A. Vorontsov, J. Mod. Opt. **43**, 93 (1996); M. A. Vorontsov and A. Yu. Karpov, J. Opt. Soc. Am. B **14**, 34 (1997).
[3] M. Le Berre, D. Leduc, E. Ressayre, and A. Tallet, Phys. Rev. Lett. **54**, 3428 (1996).
[4] E. Pampaloni, S. Residori, S. Soria, and F. T. Arecchi, Phys. Rev. Lett. **78**, 1042 (1997).
[5] M. Silber and M. R. E. Proctor, Phys. Rev. Lett. **81**, 2450 (1998).
[6] H. Arbell and J. Fineberg, Phys. Rev. Lett. **81**, 4384 (1998); **84**, 654 (2000); **85**, 756 (2000).
[7] C. Wagner, H. W. Muller, and K. Knorr, Phys. Rev. Lett. **83**, 308 (1999).
[8] H.-J. Pi, S.-Y. Park, J. Lee, and K. J. Lee, Phys. Rev. Lett. **84**, 5316 (2000).
[9] S. L. Lachinova and W. Lu, J. Opt. B: Quantum Semiclassical Opt. **2**, 393 (2000).
[10] J. Hegseth, J. M. Vince, M. Dubois, and P. Berge, Europhys. Lett. **17**, 413 (1992).
[11] G. Giacomelli, R. Meucci, A. Politi, and F. T. Arecchi, Phys. Rev. Lett. **73**, 1099 (1994).
[12] D. Raitt and H. Riecke, Physica D **82**, 79 (1995).
[13] S. Ciliberto, E. Pampaloni, and C. Perez-Garcia, Phys. Rev. Lett. **61**, 1198 (1988); E. Pampaloni, C. Perez Garcia, L. Albavetti, and S. Ciliberto, J. Fluid Mech. **234**, 393 (1992).
[14] W. J. Firth and A. J. Scroggie, Europhys. Lett. **26**, 521 (1994).
[15] R. Neubecker, G.-L. Oppo, B. Thuering, and T. Tschudi, Phys. Rev. A **52**, 791 (1995).
[16] S. Residori, P. L. Ramazza, E. Pampaloni, S. Boccaletti, and F. T. Arecchi, Phys. Rev. Lett. **76**, 1063 (1996).
[17] E. Grosse Westhoff, V. Kneisel, Yu. A. Logvin, T. Ackemann, and W. Lange, J. Opt. B: Quantum Semiclassical Opt. **2**, 386 (2000).
[18] M. A. Vorontsov, G. W. Carhart, and R. Dou, J. Opt. Soc. Am. B **17**, 266 (2000).
[19] R. Herrero, E. Grosse Westhoff, A. Aumann, T. Ackemann, Yu. A. Logvin, and W. Lange, Phys. Rev. Lett. **82**, 4627 (1999).
[20] W. Lu and S. L. Lachinova, Phys. Rev. A **63**, 013807 (2001).